Fine tuning the charge transfer in carbon nanotubes via the interconversion of encapsulated molecules

H. Shiozawa,[1,*] T. Pichler,[1,†] C. Kramberger,[1] A. Grüneis,[1] M. Knupfer,[1] B. Büchner,[1] V. Zólyomi,[2,3] J. Koltai,[3] J. Kürti,[3] D. Batchelor,[4] and H. Kataura[5]

[1]*IFW Dresden, P.O. Box 270116, D-01171 Dresden, Germany*

[2]*Research Institute for Solid State Physics and Optics of the Hungarian Academy of Sciences, P.O. Box 49, H-1525, Budapest, Hungary*

[3]*Department of Biological Physics, Eötvös University, Pázmány Péter sétány 1/A, H-1117 Budapest, Hungary*

[4]*Universität Würzburg, BESSY II, D-12489 Berlin, Germany*

[5]*Nanotechnology Research Institute, AIST, Tsukuba 305-8562, Japan*

(Received 15 December 2007; published 2 April 2008)

Tweaking the properties of carbon nanotubes is a prerequisite for their practical applications. Here, we demonstrate fine tuning the electronic properties of single-wall carbon nanotubes via filling with ferrocene molecules. The evolution of the bonding and charge transfer within the tube is demonstrated via chemical reaction of the ferrocene filler ending up as secondary inner tube. The charge transfer nature is interpreted well within density functional theory. This work gives a direct observation of a fine-tuned continuous amphoteric doping of single-wall carbon nanotubes.

DOI: 10.1103/PhysRevB.77.153402 PACS number(s): 73.22.−f, 71.15.Mb, 78.70.Dm, 79.60.−i

Encapsulation of molecules inside single-wall carbon nanotubes (SWCNTs) is of great research interest. This process generates unique one-dimensional molecular nanostructures that have a large potential to bring forth novel electronic and magnetic properties. After the pioneering works of filling with C_{60} and other fullerenes or fullerene derivatives,[1–4] organic molecules are becoming promising candidates as a functional filler.[5–7] Since their π conjugated orbital states are highly sensitive to the chemical environments, the incorporated organic molecules can greatly modify the properties of the SWCNT. Specifically, organometallics are in the focus of attention as a filling material due to their large variation of the chemical properties depending on the metal atom species. Recent theoretical studies on metallocene filled SWCNT highlighted that the variety of the metal center in between two planar aromatic ligands yields tunable carrier doping of SWCNT.[8–10] Experimentally, the encapsulation of cobaltocene[11] ($CoCp_2$) and ferrocene[12,13] ($FeCp_2$) has been so far observed with high-resolution transmission electron microscopy (HRTEM). Tube-diameter selective filling and resulting energy shifts of the corresponding fluorescence peaks were observed for the cobaltocene filled SWCNT ($CoCp_2$@NT). The HRTEM studies on a $FeCp_2$@NT reported the conversion of the $FeCp_2$@NT to double-wall carbon nanotubes[12] (DWCNTs) or to iron clusters.[13,14] These experimental works using tube materials synthesized by arc-discharge[12–14] or high-pressure CO conversion (HiPCO) methods[11] allowed one to probe the local properties of a certain type of individual filled tubes. However, it has been highly challenging to obtain a bulk-scale filling of SWCNTs with a defined diameter distribution, in order to get further insight into the bulk electronic and chemical properties and to check up the theoretical predictions.[8–10] Very recently, the bulk-scale encapsulation of $FeCp_2$ inside SWCNTs was accomplished and an extended use of filled nanotubes in nanochemistry was proposed: The reaction process of $FeCp_2$ filler precursors toward secondary inner tube growth was identified and controlled on a bulk scale.[15]

In the present work, using advantages of state-of-the-art core-level spectroscopy and $FeCp_2$@NT with a high purity and filling, we prove that the reaction process of the filler molecule can be utilized for tuning the properties of SWCNT on a bulk scale. The evolution of the chemical composition of the filler during the conversion to DWCNT is traced by observing the iron core-level absorption. The Fe $2p$ absorption spectra show a clear sign of encapsulated $FeCp_2$ and their decomposition by vacuum annealing, which is complementary to the previous photoemission and HRTEM study.[15] The C $1s$ core photoemission and absorption study unravels interactions between nanotube carbon atoms and filler molecules in the $FeCp_2$@NT, which diminish with the decomposition of $FeCp_2$. Further, a fully continuous amphoteric doping of SWCNT is realized via chemical reactions of the filler, which is evidenced by tracing Van Hove singularity (VHS) peaks in valence-band photoemission. Both n-type and p-type dopings of the outer tube are observed as bipolar energy shifts of the VHS peaks relative to those for the pristine SWCNT. A comprehensive analysis of the charge distribution within the $FeCp_2$@NT and the empty DWCNT gives very good agreement between experiment and theory. This work unveils the bonding and charge-transfer-type interactions between carbon nanotubes and filler molecules and the use of chemical reactions of encapsulated molecules in tuning the functional properties of SWCNT. This paves the way toward nanoscale electronic devices based on endohedrally functionalized carbon nanotubes.

The $FeCp_2$@NT films with a bulk filling factor of about 35% were prepared according to the previous work[15] using the laser ablation SWCNT material with tube diameters of 1.4 ± 0.1 nm.[16] A conversion of the $FeCp_2$@NT to the iron doped DWCNT was carried out via annealing at 600 °C in vacuum. In a similar way, the same batch of the $FeCp_2$@NT was transformed into empty DWCNT by annealing at 1150 °C for 1 h. The ultra violet photoemission spectroscopy was performed with monochromatic He I radiation (21.22 eV) using a hemispherical SCIENTA SES 200 photoelectron energy analyzer. The experimental resolution (better

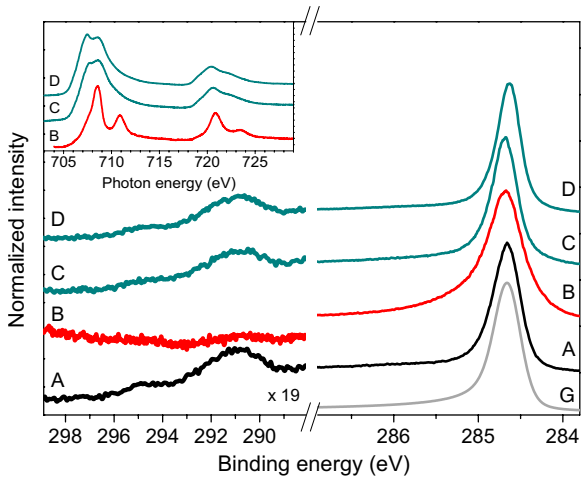

FIG. 1. (Color online) C 1*s* photoemission spectra for samples (A) SWCNT, (B) $FeCp_2$@NT, (C) Fe doped DWCNT (600 °C for 2 h), and (D) Fe doped DWCNT (600 °C for 22 h). Gray (G) is a Doniach-Sunjic profile convoluted with Gaussian, reproducing well the C 1*s* peak of the SWCNT. Inset: Fe 2*p* absorption spectrum for samples B, C, and D.

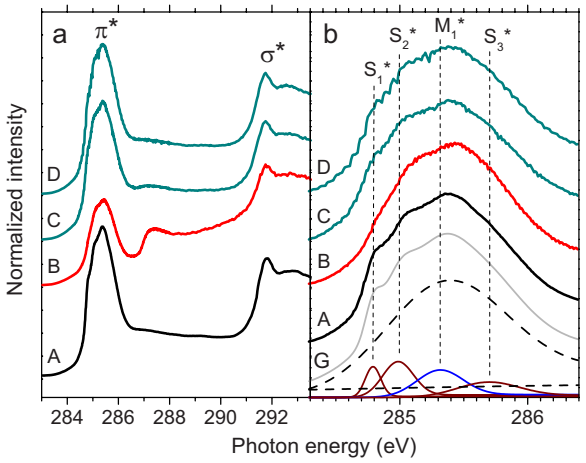

FIG. 2. (Color online) (a) C 1*s* absorption spectra for the samples (A) SWCNT, (B) $FeCp_2$@NT, (C) Fe doped DWCNT (600 °C for 2 h), and (D) Fe doped DWCNT (600 °C for 22 h). (b) Van Hove singularity peaks at π^* resonance edge on an expanded scale. Gray (G) shows the result of line shape analysis for the SWCNT (Ref. 19).

than 20 meV) and the Fermi energy were determined from the Fermi edge of clean molybdenum substrates. The x-ray absorption experiment was carried out at beamline UE 52 PGM, Bessy II. Either drain current or partial electron yield was collected with an overall resolving power better than 10 000. The base pressure in the setup was kept below 5×10^{-10} mbar. Calculations were performed using density functional theory in the local density approximation with the VASP package.[17] The cutoff energy of the plane-wave basis set was set to 350 eV. Geometry optimizations were performed until the forces on all atoms were below 0.003 eV/Å. Atomic Bader charges were evaluated using an external utility.[18]

The Fe 2*p* absorption traces the chemical environment of the iron atoms. The inset of Fig. 1 compares the Fe 2*p* absorption spectra between the pristine $FeCp_2$@NT sample (spectrum B) and the iron doped DWCNT samples (C and D). For the $FeCp_2$@NT, four discernible peaks characteristic to the molecular states of $FeCp_2$ are observed. This is very similar to the spectrum for pristine $FeCp_2$ observed previously[20] and evidences the $FeCp_2$ molecules encapsulated without decompositions or significant modifications in structure. The iron doped DWCNT samples, in turn, show a broad and asymmetric doublet composed of a set of doublets corresponding to variant chemical compositions of iron. Such a drastic change in the Fe 2*p* absorption is a direct observation of decomposition of the $FeCp_2$ molecules.

Further, the C 1*s* photoemission and absorption uncover the nature of nanotube–$FeCp_2$ interactions.[21] Both distinguish π and σ states of nanotube carbon sp^2 network. The former (latter) lies normal (parallel) to the sp^2 hexagonal plane. The main panel of Fig. 1 shows the C 1*s* photoemission spectra for the SWCNT (spectrum A), $FeCp_2$@NT (spectrum B), and Fe doped DWCNT samples (spectra C and D). The C 1*s* main peak of the $FeCp_2$@NT is obviously broader and more asymmetric than that of the SWCNT. This feature is better recognized by fitting them to the Doniach-Sunjic profile. The derived width and asymmetric parameters are 0.175 and 0.147, respectively, which are factors of 1.83 and 1.38 larger than those for the SWCNT. In turn, those for the Fe doped DWCNT samples almost recover the values for the SWCNT. Interestingly, this anomaly of $FeCp_2$@NT is concomitant to a decrease of the π plasmon peak located around 291 eV binding energy in the shake up region, possibly indicating reduced π components. This is further investigated with the C 1*s* absorption plotted in Fig. 2(a). The C 1*s* absorption spectrum for the pristine SWCNT exhibits π^* resonance peak located at a photon energy around 285.4 eV and σ^* resonance structures above 291.8 eV. In the π^* peak plotted on the expanded scale in Fig. 2(b), the fine structures corresponding to the VHS are observed for all the samples. Those are reproduced well by the line shape analysis according to the previous work,[19] as depicted at the bottom of Fig. 2(b). This observation confirms the high purity of the samples. The C sp^2 feature consisting of the π^* and σ^* structures is drastically modified in the $FeCp_2$@NT. The π^* peak intensity relative to the σ^* structures is strongly reduced and a new peak appears at 287 eV for the $FeCp_2$@NT (spectrum B). This originates from the $FeCp_2$ molecule which has a main peak structure at 287 eV corresponding to C-H bonds.[22] It should be noted, however, that there must be much less pronounced features of the raw $FeCp_2$ observed accounting for the estimated concentration of the $FeCp_2$ consisting carbons.[15] In addition to the reduced π^* peak intensity, therefore, this can be attributed to the nanotube carbon valence states modified by $FeCp_2$ adsorption on the inner wall so as to project the spectral weight of the filler molecule on the C 1*s* absorption. The diminished fraction of the π^* peak is transferred to this additional peak. This also indicates stronger interaction between $FeCp_2$ π conjugated orbital and nanotube π orbital, which is rationalized in terms of the geometry of the π and σ orbitals within the tube. Therefore, orbital mixing of the nanotube π and $FeCp_2$ π conjugated

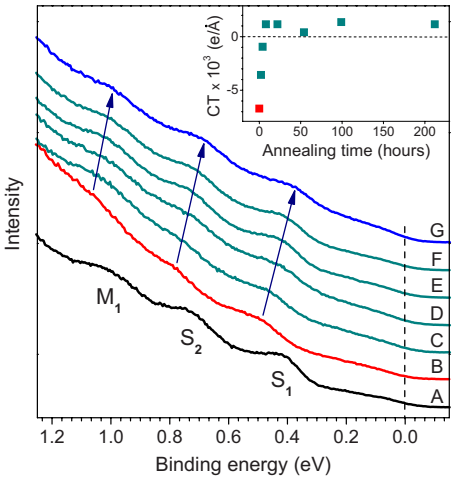

FIG. 3. (Color online) He I photoemission spectra for (A) pristine SWCNT, (B) $FeCp_2$@NT, [(C)–(F)] Fe doped DWCNT or $FeCp_2$@NT annealed at 600 °C for 2, 8, 54, and 212 h, respectively, and (G) $FeCp_2$@NT annealed at 1150 °C for 1 h. Inset: annealing time dependence of charge transfer density (CT) for the outer tube in units of $e/Å$.

orbitals must be responsible for this feature. This can cause a significant modification of the nanotube valence states. The features are very similar to those observed previously for hydrogenated or oxidized SWCNT.[23] In general, the additional bonding to the nanotube wall yields more sp^3-like carbon atoms, which results in reducing the π dominant signal.[24] This also explains the reduced π plasmon shake up in the C 1*s* photoemission of the $FeCp_2$@NT. Additionally, those sp^3-like features observed in both photoemission and absorption diminish rapidly after 2 h of annealing (spectra C and D in Figs. 1 and 3), indicating the detachment of those bonding as a consequence of the decomposition of the $FeCp_2$ molecule as observed with the Fe 2*p* absorption.

We now turn to investigate the degree of charge transfer between the tube and the filler material. This is done by observing the VHS peaks in photoemission.[21] The valence-band photoemission spectrum of the pristine SWCNT exhibits three peaks corresponding to the VHS of semiconducting tubes (S_1,S_2) and metallic tubes (M_1),[25] as shown in Fig. 3, spectrum A. For the $FeCp_2$@NT (spectrum B), those peaks are significantly shifted toward higher binding energies. From a close similarity to alkali metals doped SWCNT materials,[26,27] this behavior is safely attributed to the electron charge transfer from the $FeCp_2$ to SWCNT. Upon annealing at 600 °C (spectra C, D, E, and F), the VHS peaks are gradually shifted toward lower binding energies and become stable after 22 h. Interestingly, the reached energy positions are lower than those for the pristine SWCNT. At this stage, the material is transformed into the iron doped DWCNT.[15] In turn, upon 1150 °C annealing, we get the empty DWCNT, without any iron atoms, whose VHS peaks are further shifted toward lower energies (spectrum G). This yields a significant conclusion that there is electron transfer from the outer tube to the inner tube in the empty DWCNT. The direction of the charge transfer is the same as reported in a recent theoretical work.[28,29] Moreover, the difference between the empty DWCNT (spectrum G) and the iron doped DWCNT (spectrum F) highlights electron charge transfer from the iron materials to the outer tubes. This electron doping should be both to the inner and outer tubes, and the averaged doping level observed as VHS peak shifts depends on the chemical composition of fillers.

Finally, a quantitative analysis of the charge transfer between the filler and the SWCNT is given both experimentally and theoretically. The number of electrons transferred from the fillers to the SWCNT was evaluated from the filling factor and the VHS peak shifts by comparing them with the ones for potassium doped SWCNT. The inset of Fig. 3 shows the charge transfer density (CT) of the outer tube along the tube axis for $FeCp_2$@NT samples annealed at 600 °C for different durations. The CT has a maximum negative value of $-0.0067\ e/Å$ for the pristine $FeCp_2$@NT and drops rapidly at the first few annealing steps and becomes positive constant around $+0.0010\ e/Å$ after 8 h of annealing. In contrast, the iron concentration is much less dependent on annealing and shows only a factor of 0.7 drop in the end. These features suggest that the chemical status of the filler material is certainly responsible for the evolution of the CT. For the representative two filled samples, $FeCp_2$@NT and the empty DWCNT, the possible filled structures are available; thus, the CT for the actual samples can be extrapolated to those for 100% filled materials. The results are $-0.0180\ e/Å$ for $FeCp_2$@NT and $+0.0286\ e/Å$ for DWCNT.

On the theoretical side, we have calculated the CT between ferrocene and a host (9,9) nanotube. This tube has a diameter which is a good representation of our experimental sample and is highly suited for optimal ferrocene filling. We have examined both the standing and lying geometries of $FeCp_2$@(9,9). In the former (latter) case, the Cp-Fe-Cp axis is aligned perpendicular (parallel) to the nanotube axis. The geometries of the nanotube and the $FeCp_2$ were optimized separately, and the optimal distance between them was obtained by finding the minimum of the total energy as a function of the distance. A full geometry optimization was performed subsequently, but no essential change was found in the CT values. Both ferrocene alignments yielded a transfer of electrons from the $FeCp_2$ to the nanotube, in full agreement with the measurements. For the standing and lying geometries, the CT was found to be -0.0020 and $-0.0029\ e/Å$, respectively, far less than the experimental $-0.0180\ e/Å$. In comparison, we have also calculated the CT for the case of the (4,4)@(9,9) DWCNT, which yielded $+0.0065\ e/Å$. Once again, the direction of the charge transfer is in full agreement with the experiment, and in this case the magnitude is also closer. A previous study[28,29] has revealed that the intermolecular Hückel model[30] yields about a factor of 2 larger magnitude for the CT in double-wall tubes than the LDA does. In the case of the (4,4)@(9,9), the CT is found to be $+0.0138\ e/Å$ with this model. The latter value is much closer to the experimental value of $+0.0286\ e/Å$.

In the case of the ferrocene filled tubes, even applying a factor of 2 correction yields far too low CT. This discrepancy might suggest that the $FeCp_2$ effectively binds into the tube wall: The theoretically considered scenario, i.e., van der Waals distance between the $FeCp_2$ and the nanotube wall, allows only for weak intermolecular interactions leading to

small CT, while a strong—possibly covalent—bonding may allow for a larger CT between the two subsystems. We have performed further LDA calculations to examine this possibility by studying a simple test geometry in the parallel orientation where the two hydrogens nearest to the tube wall are removed from the $FeCp_2$ which then binds into the wall.[31] We found that in this geometry the CT is increased by around 50%, and the carbon atoms of the nanotube which are involved in the bonding are of largely sp^3 character. The latter also agrees with the aforementioned C 1*s* core-level measurements which showed reduced π characters, indicative of orbital hybridization between the subsystems. Thus, both (i) the discrepancy between the measured and calculated CT and (ii) the sp^3 character of carbon atoms found by C 1*s* spectroscopy suggest in unison that there should be some kind of covalent bonding between the $FeCp_2$ and the host nanotube. This is essentially an indication of endohedral functionalization of the nanotube, which has been suggested to be theoretically possible recently.[32]

In summary, we have evidenced the potential of filling and subsequent chemical reactions to tune the properties of SWCNT. Both *n*-type and *p*-type dopings of the SWCNT were achieved from different chemical states of the filler. Good agreement between the experimental and theoretical results shows the importance of both covalent and noncovalent interactions between the subsystems. Our combined experimental and theoretical approaches to the physics behind the chemical reaction at the nanoscale will have a large potential as a fundamental model base for exploring the nanomaterial design.

H.S. acknowledges support from the Alexander von Humboldt Foundation. C.K. acknowledges the IMPRS. A.G. acknowledges the European Union. V.Z. acknowledges the János Bolyai Foundation. We thank the DFG PI 440/3/4, OTKA (Grants Nos. K60576 and F68852) and the Ministry of Education, Culture, Sports, Science and Technology of Japan (Grant-in-Aid for Scientific Research A, No. 18201017) for financial support. We thank R. Hübel, S. Leger, R. Schönfelder, and H. Klose for technical assistance.

*Corresponding author. Present address: Advanced Technology Institute, University of Surrey, Guildford GU2 7XH, United Kingdom.

†Present address: Institut für Materialphysik, Universität Wien Strudlhofgasse 4, 1090 Wien, Austria.

[1] B. W. Smith, M. Monthioux, and D. E. Luzzi, Nature (London) **396**, 323 (1998).

[2] S. Bandow, M. Takizawa, K. Hirahara, M. Yudasaka, and S. Iijima, Chem. Phys. Lett. **337**, 48 (2001).

[3] H. Shiozawa *et al.*, Phys. Rev. B **73**, 075406 (2006).

[4] H. Shiozawa, H. Rauf, T. Pichler, M. Knupfer, M. Kalbac, S. Yang, L. Dunsch, B. Büchner, D. Batchelor, and H. Kataura, Phys. Rev. B **73**, 205411 (2006).

[5] T. Takenobu, T. Takano, M. Shiraishi, Y. Murakami, M. Ata, H. Kataura, Y. Achiba, and Y. Iwasa, Nat. Mater. **2**, 683 (2003).

[6] Y. Fujita, S. Bandow, and S. Iijima, Chem. Phys. Lett. **413**, 410 (2005).

[7] K. Yanagi, Y. Miyata, and H. Kataura, Adv. Mater. (Weinheim, Ger.) **18**, 437 (2006).

[8] J. Lu, S. Nagase, D. P. Yu, H. Q. Ye, R. S. Han, Z. X. Gao, S. Zhang, and L. M. Peng, Phys. Rev. Lett. **93**, 116804 (2004).

[9] V. M. Garcia-Suaez, J. Ferrer, and C. J. Lambert, Phys. Rev. Lett. **96**, 106804 (2006).

[10] E. L. Sceats and J. C. Green, J. Chem. Phys. **125**, 154704 (2006).

[11] L. J. Li, A. N. Khlobystov, J. G. Wiltshire, G. A. D. Briggs, and R. J. Nicholas, Nat. Mater. **4**, 481 (2005).

[12] L. H. Guan, Z. J. Shi, M. X. Li, and Z. N. Gu, Carbon **43**, 2780 (2005).

[13] Y. F. Li, R. Hatakeyama, T. Kaneko, and T. Okada, Jpn. J. Appl. Phys., Part 2 **45**, L428 (2006).

[14] Y. F. Li, R. Hatakeyama, T. Kaneko, T. Izumida, T. Okada, and T. Kato, Nanotechnology **17**, 4143 (2006).

[15] H. Shiozawa, T. Pichler, A. Grüneis, R. Pfeiffer, H. Kuzmany, Z. Liu, K. Suenaga, and H. Kataura, Adv. Mater. (Weinheim, Ger.) (to be published).

[16] H. Kataura, Y. Maniwa, M. Abe, A. Fujiwara, T. Kodama, K. Kikuchi, H. Imahori, Y. Misaki, S. Suzuki, and Y. Achiba, Appl. Phys. A: Mater. Sci. Process. **74**, 349 (2002).

[17] G. Kresse and J. Furthmuller, Phys. Rev. B **54**, 11169 (1996).

[18] G. Henkelman, A. Arnaldsson, and H. Jonsson, Comput. Mater. Sci. **36**, 354 (2006).

[19] C. Kramberger, H. Rauf, H. Shiozawa, M. Knupfer, B. Buchner, T. Pichler, D. Batchelor, and H. Kataura, Phys. Rev. B **75**, 235437 (2007).

[20] A. P. Hitchcock, A. T. Wen, and E. Rühl, Chem. Phys. **147**, 51 (1990).

[21] The carbon signal from the filler material is not observable due to the number of carbon atoms much smaller than for the SWCNT.

[22] E. Rühl and A. P. Hitchcock, J. Am. Chem. Soc. **111**, 5069 (1989).

[23] A. Nikitin, H. Ogasawara, D. Mann, R. Denecke, Z. Zhang, H. Dai, K. Cho, and A. Nilsson, Phys. Rev. Lett. **95**, 225507 (2005).

[24] J. Stöhr, *NEXAFS Spectroscopy* (Springer-Verlag, Berlin, 1992).

[25] H. Ishii *et al.*, Nature (London) **426**, 540 (2003).

[26] H. Rauf, T. Pichler, M. Knupfer, J. Fink, and H. Kataura, Phys. Rev. Lett. **93**, 096805 (2004).

[27] R. Larciprete, L. Petaccia, S. Lizzit, and A. Goldoni, Phys. Rev. B **71**, 115435 (2005).

[28] V. Zólyomi, Á. Rusznyák, J. Kürti, Á. Gali, F. Simon, H. Kuzmany, Á. Szabados, and P. R. Surján, Phys. Status Solidi B **243**, 3476 (2006).

[29] V. Zólyomi, J. Koltai, Á. Rusznyák, J. Kürti, Á. Gali, F. Simon, H. Kuzmany, Á. Szabados, and P. R. Surján, arXiv:cond-mat/0603407 (unpublished).

[30] A. Lázár, P. R. Surján, M. Paulsson, and S. Stafström, Int. J. Quantum Chem. **84**, 216 (2001).

[31] This test geometry is energetically unfavorable. In the real system, instead, we expect that the $FeCp_2$ binds into the wall at defect sites. This will be explored in more detail in a future work.

[32] T. Yumura and M. Kertesz, Chem. Mater. **19**, 1028 (2007).